In vivo toxicity of nano-alumina on mice neurobehavioral profiles and the potential mechanisms

Article *in* International journal of immunopathology and pharmacology · January 2011

Source: PubMed

CITATIONS
43

READS
221

9 authors, including:

Qilin Zhang

84 PUBLICATIONS **346** CITATIONS

SEE PROFILE

Curry Zhang

University of Science and Technology Beijing

240 PUBLICATIONS **2,348** CITATIONS

SEE PROFILE

Qiao Niu

Shanxi Medical University

136 PUBLICATIONS **1,058** CITATIONS

SEE PROFILE

INTERNATIONAL JOURNAL OF IMMUNOPATHOLOGY AND PHARMACOLOGY Vol. 24, no. 1, (S) 23-29 (2011)

IN VIVO TOXICITY OF NANO-ALUMINA ON MICE NEUROBEHAVIORAL PROFILES AND THE POTENTIAL MECHANISMS

Q.L. ZHANG, M.Q. LI, J.W. JI, F.P. GAO[1], R. BAI[2], C.Y. CHEN[2], Z.W. WANG, C. ZHANG, and Q. NIU

Department of Occupational Health, School of Public Health, Shanxi Medical University Taiyuan, People's Republic of China; [1]Technical Institute of Physics and Chemistry, Chinese Academy of Sciences, Beijing, People's Republic of China[2]National Central of Nanoscience and Technology, Beijing, People's Republic of China

The rapid development and expanding applications of nanotechnology have led to enhanced exposure of human body to nanoparticles. It is, therefore, necessary to address the safety issue via rigorous toxicological evaluation and to understand the underlying interaction mechanism. However, only a few studies to date have evaluated the safety of nano-sized materials and their potential adverse effects on biological systems. In this study, we sought to investigate the potential toxicity of aluminum oxide (alumina) nanoparticles in ICR strained mice, focusing on potential neurobehavioral defects and the possible mechanisms. The results demonstrated that nano-alumina impaired neurobehavioral functions, including lengthened escape latency, shorter time spent in the target quadrant and reductions in the number of platform crossing. In addition, it induced cell necrosis and apoptosis, which were likely mediated by the reduction of MMP and ROS, and the induction of the caspase-3 gene. Our results implicated that mitochondrial impairment plays a key role in neurotoxicity of nano-alumina, sequent oxidative damage and neural cell loss, especially necrosis, may be direct causes for the neurobehavioral defects. Collectively, nano-alumina presents a strong pro-cell death effect on ICR mice in vivo, suggesting that nano-alumina may serve as an inducer for neural toxicology. Findings in the present study indicating that surface chemical characteristics and nanoscale sizes of nano-alumina could co-contribute significantly to neurotoxicity. The impaired neurobehavioral patterns indicate that nano-alumina particles are more toxic to the cerebrum than those of nano-carbon with the same nanoparticle size and micro-alumina with the same surface chemical characteristics.

It is well established that aluminum (Al) is a neurotoxic agent (1-3) which has been associated with several neurodegenerative diseases, such as dialysis encephalopathy, amyotrophic lateral sclerosis, parkinsonism dementia, and in particular, Alzheimer's disease (4-7). In fact, it has been stated that the use of Al as an experimental neurotoxicant has recapitulated virtually every feature of the neurodegenerative spiral afflicting Alzheimer's patients, such as accumulation of tau protein and amyloid-beta protein, and induction of neuronal cell death (8-10). Additional evidence suggests that various mechanisms have been proposed for Al-induced neurotoxicity, including free radical damage via enhanced lipid peroxidation, impaired glucose metabolism, effects on signal transduction and protein modification, alterations on the axonal transport, and alteration of phosphorylation levels of neurofilaments (11-14).

In recent years, nanoparticles have generated profound impacts on industry, environment and human health, largely due to their unique physical and chemical characteristics. Nano-alumina, or aluminum oxide nanoparticle, is among the most abundantly produced nanosized particles, accounted for approximately 20% of the 2005 worldmarket of nanoparticles (15). Engineered nanoparticle production rates have been anticipated to increase to 58,000 metric tons produced per year by the year 2011 (16). Given that nano-alumina has been widely used for commercial purposes and its potential neurotoxicity, further research into the neurotoxicity of this nanoparticle is both warranted and essential.

Key words: Alumina nanoparticles, mice, neurobehavioral defects , apoptosis

Mailing address: Prof. Qiao Niu, MD, MS, PhD
Prof. Qinli Zhang, MD, MS, PhD
Department of Occupational Health,
School of Public Health,
Shanxi Medical University, Taiyuan, 030001, China
Tel: ++86 351 4135029 Fax: ++86 351 2027943
e-mail: niuqiao55@163.com; zhangql930611@126.com

0394-6320 (2011)

MATERIALS AND METHODS

Preparation of the nanoparticles and their charateristics

Nanoparticles and microparticles were purchased from Sigma-Aldrich (St. Louis, MO, USA), they were nano-alumina (Nano-Al, gamma phase, nanopowder, <50 nm); nano-carbon (Nano-C, nanopowder, <50 nm particle size (BET), ≥99% trace metals basis); and aluminum oxide (Micro-Al, powder,10 μm, 99.7% trace metals basis).

All the particles have been prepared according to a previously described method (17). The nanoparticle dispersion was characterized by using a particle size distribution (PSD) analyzer, transmission electron microscopy (TEM), and electron diffraction. For the PSD, nanoparticles were dispersed in the media and vortexed. Subsequently, 5ml of the dispersion was added to a quartz cuvette, and placed in the Brookhaven 90Plus Nanoparticle size analyzer (Brookhaven Instruments, Holtsville, NY). Fluctuations of the scattered light due to the random motion of the particles fluctuations were measured and converted into particle diameter. For the TEM, a drop of the nanoparticle suspension was placed on a 200 mesh Cu-lacy carbon TEM grid (EM Sciences, Hatfield, PA), which was allowed to dry overnight in a vacuum oven at room temperature. After evaporation, the alumina nanoparticles were dispersed on the TEM grid. TEM measurements were performed in a JEOL 2010f instrument (JEOL, Tokyo, Japan) with operating voltage of 200 kV. The electron diffraction experiment was performed on the same sample used for TEM. The diffraction pattern and indexing was obtained using Digital Micrograph Imaging Software (Gatan, Pleasanton, CA) interfaced with the microscope.

Experimental animals and treatment

All manipulations of animals conformed to the guidelines provided by the National Institutes of Health in *Guide for the Care and Use of Laboratory Animals*. Male ICR mice (30–35 g each) were purchased from the Laboratory Animal Center of Chinese Academy of Sciences (Beijing, China). Mice were group housed and maintained on a 12-h light/dark cycle with *ad libitum* access to food and water. The mice were inoculated intranasally (i.n.) per day with Nano-Al, Nano-C and Micro-Al at the dose of 100 mg/kg as the experimental groups, mice received 0.9% saline were used as controls. The mice were sacrificed 10 d post-inoculation.

Morris water maze analysis

The Morris water maze (MWM) task was performed essentially as described previously (18) with minor modifications. Briefly, each mouse underwent daily sessions of 4 trials for 4 consecutive days. For each trial, a mouse was released into water facing the wall at one of the four standard start locations selected at random. When succeeded in locating the platform, it was allowed to stay on the platform for 15 s. If the mouse failed to find the platform within 120 s, it was assisted by the experimenter and allowed to stay there for the same time. The trials were conducted in blind as the experimenters did not know the group assignments. All trials were videotaped by a camera located 2 m above the water surface; the swimming speed, the time required to find the hidden platform, the time spent in the target quadrant and the number of crossing were recorded. The interval between trials was 20 min. A probe trial was performed 24 h after the last training session. In this trial, the platform was removed from the tank and the mice were allowed to swim freely for 120s. The time spent in the target quadrant and the number of crossing over the platform site was recorded to indicate the degree of memory consolidation after learning.

Flow cytometry assay

The cell death rate was detected using an Annexin V-FITC apoptosis detection kit (BD Biosciences Pharmingen, San Diego, CA). The cells in the hippocampus were trypsinized and collected. 1×10^5/ml cells were washed twice in cold PBS and resuspended in 100 μl binding buffer. 5 μl of Annexin V-FITC and 5 μl of PI were added and gently mixed, followed by incubation in the dark for 15 min. The cells were acquired within 60 min using an FACS calibur flow cytometer (BD Biosciences, CA, USA). The fluorochrome was excited using the 488 nm line of argonion laser; Annexin-V and PI emissions were monitored at 525 nm and 620 nm, respectively. A total of 20,000 events were acquired for each sample. For mitochondria membrane potential (MMP) staining, the cells were incubated with 40 nM JC-1 for 30 min at 37°C, washed once and analyzed with the FACS calibur. For reactive oxygen species (ROS) assay, the cells were incubated with 5 μM dihydrothidium (Molecular Probe) for 30 min at 37°C, washed once and analyzed with the FACS calibur.

Caspase-3 and LC3-II genes expression

Expression of caspase-3 and LC3-II genes in hippocampus of mice were analyzed with qRT-PCR. Briefly, total cellular RNA was isolated using Trizol reagent according to the instructions provided. One microgram RNA was then reverse-transcribed using oligo dT primer and 60 U of Superscript II reverse transcriptase. Real-time SYBR Green primers for caspase-3, LC3-II and GAPDH were designed using Beacon Designer (Premier, Biosoft International, Palo Alto, CA, USA). The sequences were as follows: caspase-3, forward primer 5'-CTTCCAGCCTGAGAGCAACC-3'; reverse primer 5'-CGGCGGAGGGTCAGATGG-3'; LC3-II, forward primer 5'- CTCCAGAGGTCAGGTCGTT -3', reverse primer, 5'-TGGCATAGATGGCGTTG -3'; GAPDH, forward primer 5'-ACCACAGTCCATGCCATCAC-3', reverse primer, 5'-ACCTTGCCCACAGCCTTG-3'. Template was combined with primers and 2×Taqman Universal SYBR Green PCR Master Mix in a 25 μl total reaction volume, and amplification was performed using an ABI Prism ® 7900HT sequence detection system (Applied Biosystems, USA). Cycling conditions were 2 min at 50°C, 10 min at 95°C, and 50 cycles of 92°C for 30 s and 60°C for 1 min. Real-time fluorescence detection was performed during the 60°C annealing/ extension step of each cycle. Melt-curve analysis was performed and the difference in mRNA expression among the treatment groups was determined with a relative quantification method.

Statistical analysis

Data are presented as mean ± SD of quadruplicate experimental results. Statistical analyses were performed using SPSS 10.0 software, including chi-square test for categorical

data, two-way analysis of variance (ANOVA) for the escape latency of mice in the MWM training with treatment and training day being the two factors, one-way ANOVA for group differences in the remaining measurement data, and the Student–Newman–Keuls (SNK) *t*-test as the post-hoc test. A value of $P < 0.05$ was considered statistically significant.

RESULTS

Morphology and characteristic of the nanoparticles

The nanoparticle dispersion was characterized by using a PSD analyzer, TEM, and electron diffraction. There was no change in the structural and physical characteristics of alumina nanoparticles after autoclaving. This was confirmed by TEM and electron diffraction studies before and after this process. For the characterization of Nano-Al, the particle size distribution had a range from 70.4 to 128.4 nm due to the aggregation, and the hydrodynamic mean diameter was 149.2 nm by DLS test. The values of zeta potential were 47.6; while for the characterization of Nano-C, the particle size distribution had a wide range from 36.1 to 326.2 nm due to the aggregation, and the hydrodynamic mean diameter was 194.0 nm by DLS test. The values of zeta potential were -30.4.

Effect of Nano-Al on neurobehavioral profiles

To evaluate the effects of Nano-Al on neurobehavior in mice, we first analyzed the swim speed in the first trial of the first session during the hidden platform training before mice from any of the four groups knew the location of the platform. There were no significant differences in the swim velocity among the groups, although mice in the Nano-Al treated group appeared somewhat impaired neurobehavior relative to those in the Control, Nano-C and Micro-Al treated groups (Fig. 2A). Subsequently, we used the escape latency to evaluate spatial learning and memory. Significant effects of experimental duration on the latency to locate the hidden platform were observed during the navigation training in the MWM (Fig.2B). Data in different treatment groups showed significant differences, but no interaction was found between the length and the type of treatment. The overall mean escape latency of the control was not significantly longer than that of Nano-C treated mice. However, significant difference was found in those of Micro-Al treated mice when compared with those treated with 0.9% normal saline.

During the probe trial, the Nano-Al treated mice spent significantly less time in the target quadrant when the platform was removed (Fig.2C) and exhibited fewer platform crossings (Fig.2D). In Nano-C treated group, both measurements were decreased but showed no significant difference compared with those of the control group. Comparison of data between Nano-Al and Micro-Al treated groups indicated that mice treated with Nano-Al required longer escape latency, spent less time in the target quadrant and crossed the platform fewer times

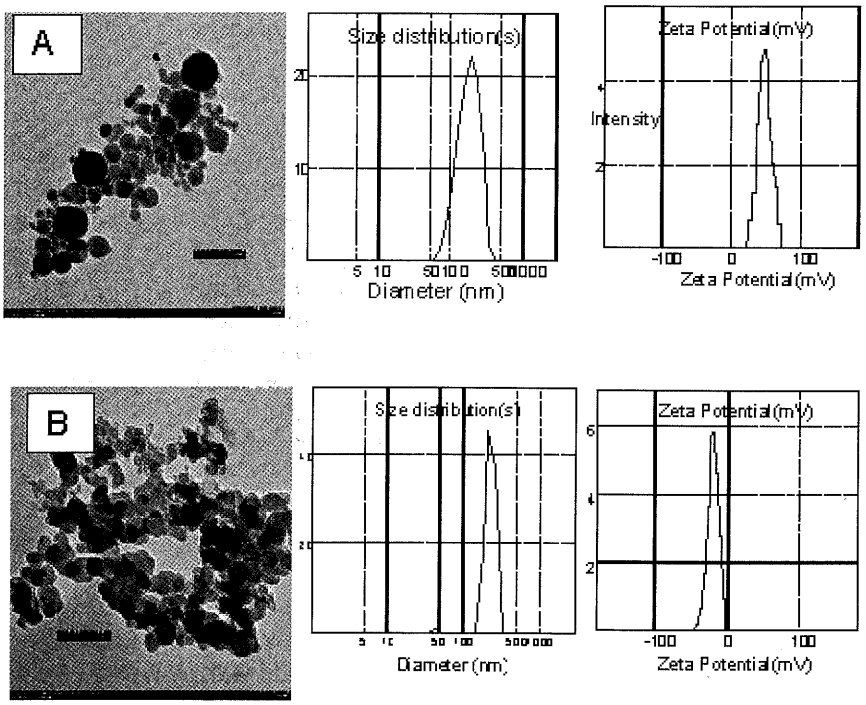

Fig. 1. *Dispersion and characterization of Nano-Al (A) and Nano-C (B) were characterzed by TEM, DSL and Zeta potential.*

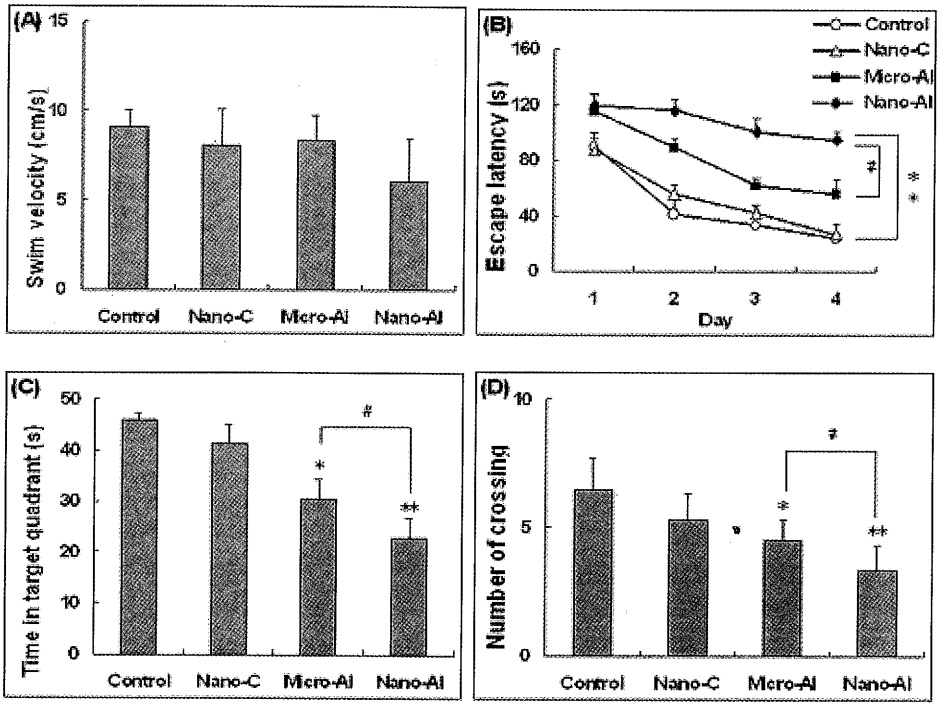

Fig. 2 *Nano-Al induced impairments of spatial learning and memory in MWM. A) Swimming speed in the first trial of the first session during the hidden platform training. B) Escape latency to reach the platform. C) Time spent in the target quadrant in the probe trial. D) Number of platform crossings in the probe trial. Bars represented Mean ± SD. * P<0.05, ** P<0.01 versus the control group. # P<0.05, versus the Nano-Al group.*

(Fig.2B,C,D).

Flow cytometry assay

To investigate the potential mechanisms by which Nano-Al impaired the neurobehavior, we focused on changes in MMP and ROS of mice hippocampus. As indicated in Fig. 3A, treatment with 100 mg/kg Nano-Al but not with the same concentration of Nano-C resulted in a highly significant decrease in MMP. Alterations in mitochondrial potential may result in induction of cellular oxidative stress (Fig. 3B). Mitochondria consume over 90% of the oxygen in the cell for ATP production; thus, the disruption of the mitochondrial respiratory chain can directly lead to lower ATP production and higher superoxide escape. Furthermore, Nano-Al mediated MMP loss and significantly higher ROS confirmed that Nano-Al may cause more severe neurotoxicity than Micro-Al do. On the other hand, Nano-C with the same nanoparticle size resulted in only mild neurotoxicity that was not significantly different from those treated by 0.9% normal saline.

It is known that an altered MMP constitutes one of the initiating events in the cell death process and cellular oxidation can also activate redox-responsive cell death. As indicated in Fig. 3C, both Nano-C and Nano-Al at 100 mg/kg were toxic and enhanced the necrotic rate, and the necrotic rate induced by Nano-Al was markedly higher than apoptotic rate. Apoptosis was also observed in Nano-Al treated mice, and became more pronounced in Micro-Al treated mice, and robust caspase-3 activation likely indicated significant apoptosis. In addition, lower expression of LC3 suggested that autophagy may not be the major cell death mode induced by Nano-C, Nano-Al and Micro-Al (Fig. 3D).

DISCUSSION

Because of the extremely increased usage of manufactured nanoparticles, occupational and public exposure to these nanoparticles will dramatically increase in the future. With this in mind, there has been a recent emergence of concern dealing with the potential for toxicity and the lack of data to substantiate or dismiss these concerns. Studies have demonstrated that manufactured aluminum oxide nanoparticles decrease expression of tight junction proteins in brain vasculature, and intracisternal injection of Nano-Al impaired the blood brain barrier. Increasing evidence suggests that oxidative

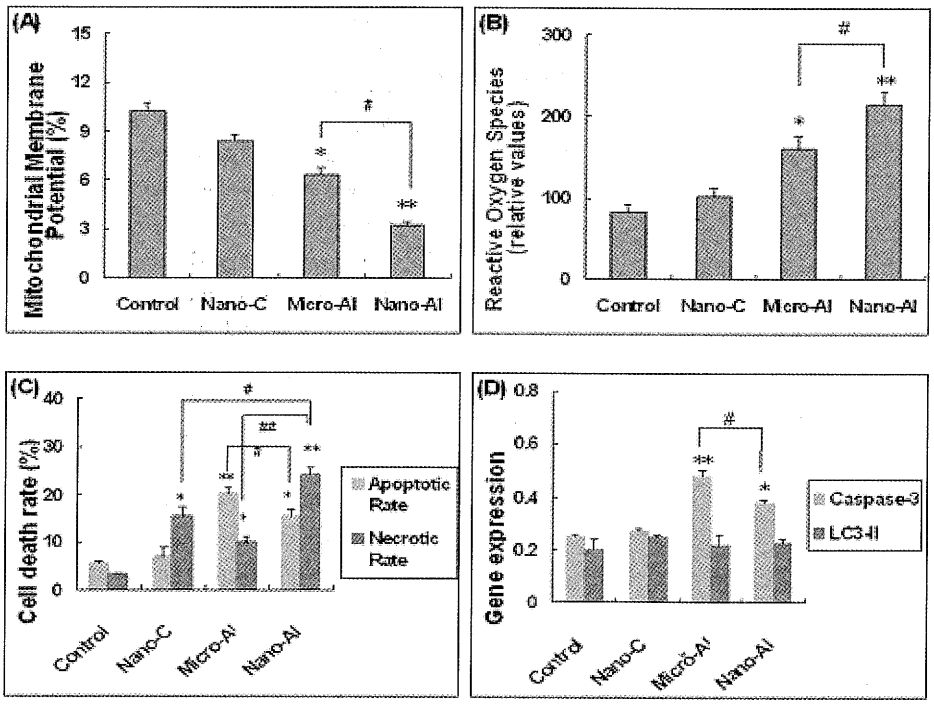

Fig. 3 *Nano-alumina induced cellular injury and cell death. A) Mitochondria membrane potential was measured using the JC-1 fluorescent probe. B) Production of superoxide was also quantified. C) The fluorescent intensity of Annexin V and PI were plotted to quantify the apoptotic and necrotic rates. D) Caspase-3 and LC3-II gene expression were compared among the groups. *: Statistical difference as compared with that of control, P<0.05; **: P<0.01. #: significant difference as compared with that of Nano-Al, P<0.05; ##: P<0.01.*

stress and apoptosis are key events in the neuropathological changes following exposure to Nano-Al (19-21).

In the present study, we observed several significant impediments during the 10-d intranasal inoculation treated with Nano-Al particles. Comparison of the swimming speed in the first trial of the first session during the hidden platform training indicated that there was no significant difference among the four groups. Based on this, two-way ANOVA with repeated measures revealed a significant effect associated with the duration and the type of treatment, yet no day & treatment interaction was observed. In addition, there were significant differences in the time spent in the target quadrant and the number of platform crossing among the groups. Post-hoc analysis indicated that both the Nano-Al and Micro-Al, but not Nano-C, groups showed deficits in performance with longer escape latency, shorter time in the target quadrant and fewer crossings compared with those of the control. Furthermore, there were significant differences between those of Nano-Al and Micro-Al groups. Collectively, such impaired neurobehavioral patterns indicated that Nano-Al particles are more toxic to the cerebrum than those of Nano-C with the same nanoparticle size and Micro-Al with the same surface chemical characteristics. It suggests that surface chemical characteristics and nanoscale sizes co-contribute to neurotoxicity of nanoparticles.

To evaluate the potential toxicity and the general mechanism involved in Nano-Al induced neurotoxicity, indicators of ROS, MMP, and cell death related gene expression are all compromised. *MMP* ($\Delta\Psi$ m), an indicator of cytotoxicity, is key to mitochondrial function and *cellular* survival; while ROS are implicated in cell damage. Marked decrease in MMP and increase in ROS levels were observed in Micro-Al treated rats, which became more pronounced in Nano-Al treated rats; while the results of Nano-C showed no significant differences from those of the control. Furthermore, ROS and mitochondria also play an important role in the induction of cell death under Nano-Al and Micro-Al conditions. Flowcytometry results indicated that apoptosis and necrosis involved in the cell death process, gene (mRNA) transcription analysis additionally clarified that apoptosis and caspase-3 gene induction were intensified in Micro-Al treated mice, which became weak in Nano-Al treated mice, while necrosis played the primary role in Nano-Al and Nano-C treated mice. Our results implicated that mitochondrial impairment plays a key role in neurotoxicity of Nano-Al, sequent oxidative damage and

neural cell loss, especially necrosis, may be direct causes for the neurobehavioral defects.

In conclusion, the present study addressed potential mechanism of neurotoxicity and revealed that Nano-Al can induce a significant neurotoxicity in animal models. The potential mechanism may intereacted with mitochondria function and cellular active oxygen, In addition, necrosis may be a primary cell death pathway involved in the neurotoxic process. Currently, our studies on acute neurotoxicity and biodistribution of alumina nanoparticles are ongoing.

ACKNOWLEDGEMENT

This study was supported by the National Natural Science Foundation of China (No. 30972512, 30972456), The Specialized Research Fund for the Postdoctoral Program (No. 200902579).

REFERENCES

1. Abd-Elghaffar S, El-Sokkary GH, Sharkawy AA. Aluminum-induced neurotoxicity and oxidative damage in rabbits: protective effect of melatonin. Neuro Endocrinol Lett 2005; 26(5): 609-16.
2. Niu PY, Niu Q, Zhang QL, Wang LP, He SE, Wu TC, Conti P, Di Gioacchino M, Boscolo P. Aluminum impairs rat neural cell mitochondria in vitro. Int J Immunopathol Pharmacol 2005; 18 (4): 683-89.
3. Kumar V, Gill KD.Aluminium neurotoxicity: neurobehavioural and oxidative aspects. Arch Toxicol 2009; 83(11):965-78.
4. Frisardi V, Solfrizzi V, Capurso C, Kehoe PG, Imbimbo BP, Santamato A, Dellegrazie F, Seripa D, Pilotto A, Capurso A, Panza F. Aluminum in the diet and Alzheimer's disease: from current epidemiology to possible disease-modifying treatment. J Alzheimers Dis 2010; 20 (1): 17-30.
5. Bharathi, Vasudevaraju P, Govindaraju M, Palanisamy AP, Sambamurti K, Rao KS. Molecular toxicity of aluminium in relation to neurodegeneration. Indian J Med Res 2008; 128 (4): 545-56.
6. Drago D, Bolognin S, Zatta P. Role of metal ions in the abeta oligomerization in Alzheimer's disease and in other neurological disorders. Curr Alzheimer Res 2008; 5 (6): 500-7.
7. Rondeau V, Jacqmin-Gadda H, Commenges D, Helmer C, Dartigues JF. Aluminum and silica in drinking water and the risk of Alzheimer's disease or cognitive decline: findings from 15-year follow-up of the PAQUID cohort. Am J Epidemiol 2009; 169 (4): 489-96.
8. Chen TJ, Hung HS, Wang DC, Chen SS. The protective effect of Rho-associated kinase inhibitor on aluminum-induced neurotoxicity in rat cortical neurons. Toxicol Sci 2010; 116 (1): 264-72.
9. Castorina A, Tiralongo A, Giunta S, Carnazza ML, Scapagnini G, D'Agata V. Early effects of aluminum chloride on beta-secretase mRNA expression in a neuronal model of beta-amyloid toxicity. Cell Biol Toxicol 2010; 26 (4): 367-77.
10. Walton JR, Wang MX. APP expression, distribution and accumulation are altered by aluminum in a rodent model for Alzheimer's disease. J Inorg Biochem 2009; 103 (11): 1548-54.
11. Rui D, Yongjian Y. Aluminum chloride induced oxidative damage on cells derived from hippocampus and cortex of ICR mice. Brain Res 2010; 1324: 96-102.
12. Garcia T, Esparza JL, Nogués MR, Romeu M, Domingo JL, Gómez M. Oxidative stress status and RNA expression in hippocampus of an animal model of Alzheimer's disease after chronic exposure to aluminum. Hippocampus 2010; 20 (1): 218-25.
13. Exley C. The pro-oxidant activity of aluminum. Free Radic Biol Med 2004; 36 (3): 380-7.
14. Gomez M, Esparza JL, Nogues MR, Giralt M, Cabre M, Domingo JL. Pro-oxidant activity of aluminum in the rat hippocampus: gene expression of antioxidant enzymes after melatonin administration. Free Radic Biol Med 2005; 38 (1): 104-11.
15. Rittner MN. Market analysis of nanostructured materials. Am Ceram Soc Bull 2002; 81: 33–6.
16. Maynard AD. Nanotechnology: Assessing the risks. Nanotoday 2006; 2: 22-33.
17. Chen L, Yokel RA, Hennig B, Toborek M. Manufactured aluminum oxide nanoparticles decrease expression of tight junction proteins in brain vasculature .J Neuroimmune Pharmacol 2008; 3 (4): 286-95.
18. Hamm RJ, Dixon CE, Gbadebo DM, Singha AK, Jenkins LW, Lyeth BG, Hayes RL. Cognitive deficits following traumatic brain injury produced by controlled cortical impact. J Neurotrauma 1992; 9: 11-20.
19. Pauluhn J. Pulmonary toxicity and fate of agglomerated 10 and 40 nm aluminum oxyhydroxides following 4-week inhalation exposure of rats: toxic effects are determined by agglomerated, not primary particle size. Toxicol Sci 2009; 109 (1): 152-67.
20. Yang K, Zhu L, Xing B. Sorption of phenanthrene by nanosized alumina coated with sequentially extracted humic acids. Environ Sci Pollut Res Int 2010; 17 (2): 410-9.
21. Doshi R, Braida W, Christodoulatos C, Wazne M, O'Connor G. Nano-aluminum: transport through sand

columns and environmental effects on plants and soil communities. Environ Res 2008; 106 (3): 296-303.